

# Penumbral finestructure: need for larger telescopes

H. BALTHASAR<sup>1</sup>, P. SÜTTERLIN<sup>2</sup> and M. COLLADOS<sup>3</sup>

<sup>1</sup> Astrophysikalisches Institut Potsdam, Telegrafenberg, D-14473 Potsdam, Germany

<sup>2</sup> Sterrenkundig Instituut Utrecht, Postbus 8000, NL-3507 TA Utrecht, The Netherlands

<sup>3</sup> Instituto de Astrofísica de Canarias, Via Lactea, E-38200 La Laguna, Tenerife, Spain

Received 2001 November 20; accepted 2001 November 21

**Abstract.** We obtained at the same time G-band images at the Dutch Open Telescope (DOT) on La Palma and spectropolarimetric data in the near infrared at the German Vacuum Tower Telescope (VTT) on Tenerife. The spectropolarimetric data show interesting correlations. Bright filaments have a smaller magnetic field strength, and higher Evershed velocities occur in dark structures. This result is in agreement with some previous observations, but also in contradiction to others. However, we suffer from the fact that the resolution limit of the VTT at a wavelength of  $1.565 \mu\text{m}$  corresponds to 400 km. Spatial power spectra derived from the DOT data indicate a typical width of 250 km for penumbral filaments. Obviously a solar telescope with an aperture of at least 1.5 m is needed to obtain sophisticated results for penumbral structures.

**Key words:** Sun: sunspots

## 1. Introduction

The radial structure of the penumbra is a phenomenon which is poorly understood up to now. Some progress was achieved with the theoretical calculations of Schlichenmaier, Jahn & Schmidt (1998) who investigated a rising flux tube in a magnetic background. A large number of observers considered relations between the intensity structure, the Doppler velocities and the magnetic field, but all ground-based observations suffer from the limited spatial resolution of the instruments and the influence of atmospheric seeing. Beckers & Schröter (1968) discussed the idea that dark structures have a higher magnetic field strength, and that dark structures are more inclined with respect to the surface normal. Later papers report different results: Schmidt et al. (1992) found indications that only the inclination of the magnetic field is different for bright and dark filaments, but other investigators found even stronger field in less inclined structures (Degenhardt & Wiehr 1991, Lites et al. 1993 or Stanchfield et al. 1997). Therefore it is still under discussion how large the actual size of a penumbral filament in the azimuthal direction is. Spatial power spectra shown by Sánchez Almeida & Bonet (1998) indicated that the noise level is not reached at their resolution limit of  $0''.28$ . Sánchez Almeida (1998) claimed that the real size must be of the order of 1 - 15 km, but Martínez Pillet (2000) presented a model calculation of flux tubes with a diameter of 100 km, embedded in a background field, which is able to explain the

observed asymmetric Stokes profiles (see also the discussion of Sánchez Almeida 2001 and Martínez Pillet 2001).

Here we present a comparison of spatially high resolution continuum images with magnetically high sensitive spectropolarimetric observations.

## 2. Observations and data reductions

The large sunspot of AR 8704 was observed on 20 September 1999 with the German Vacuum Tower Telescope (VTT) on Tenerife and with the Dutch Open Telescope (DOT) on La Palma. The spot was located at  $21^\circ$  of southern latitude at a central meridian distance of  $29^\circ$ , thus  $\cos \vartheta$  was 0.77. At the VTT we recorded the full Stokes vector of the Fe I line at  $1.5648 \mu\text{m}$  which forms a Zeeman-triplet with a splitting factor  $g_{eff} = 3.0$ . This line is thus extremely sensitive to the magnetic field. It is formed in the deep photosphere; in the quiet sun it originates below  $\lg \tau = -1$ , and due to the rather high excitation potential of 5.43 eV it stems from even deeper layers in the sunspot. We used the Tenerife Infrared Polarimeter (TIP) described by Martínez Pillet et al. (1999), one of the magnetically most sensitive polarimeters for solar physics. The full Stokes vector for a single slit position is obtained within an exposure time of 2 seconds. The observation procedure was similar to that of Balthasar et al. (2000), except that we did an extended spatial scan instead of time series. To cover the whole spot and its surroundings we needed 250 slit positions with a distance of  $0''.38$ . Along

Correspondence to: hbalthasar@aip.de

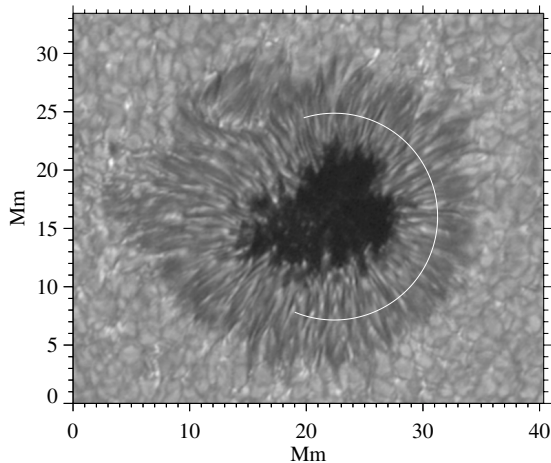


**Fig. 1.** A G-band image of the spot, obtained at the DOT. This image has been corrected for projection effects. The white line indicates the arc where the data for the spatial power spectra have been extracted.

the slit the pixel distance was  $0''.35$ . The spatial resolution limit of the telescope at this wavelength is  $0''.56$ , corresponding to 400 km, and seeing influences cause that the actually achieved resolution is about  $1''.0$ .

At the DOT we took a time series of medium-band filtergrams in the G-band around 430 nm from 14:10 to 16:40 UT. Images were obtained with a rate of approximately 10 frames per second, the one with the highest rms within 20 s was selected to be stored. The frame size was  $768 \times 572$  pixel, one pixel corresponds to  $0''.0815$ . The theoretical resolution of the DOT is  $0''.2$  at 430 nm. The following data reduction is done in a similar way as described by Sütterlin (2001). Image motion was corrected by tracking the single frames using cross correlation to the average image. The differential image motion (distorsion) was then corrected using local correlation tracking and regridding in a three-step sequence with decreasing step width. In the last step the images were corrected for the instrumental and atmospheric MTF. This was done by comparing the images in Fourier space with a ‘true’ image of the spot, which was obtained in another series earlier that day and which has been reconstructed using the speckle masking method. For this reference image the average radial power-spectrum was computed. This was also done for each image in the series, and from the quotient of the two an enhancement function was determined. Figure 1 shows an image obtained this way. Finally we corrected the geometrical foreshortening due to the position on the sun obtaining images with constant scale of 59 km in both axes.

Figure 2 shows the spot in the infrared continuum close to the selected line, this image was composed from the Stokes-I spectra obtained during the scan. The data are resized to an equal spacing of  $0''.35$  in both spatial directions, and a small tilt of  $3^\circ$  between the scan direction and the normal to the slit has been removed. The TIP-data have been taken at about 15:30 UT. Even taking the geometrical foreshortening into account, the spot exhibits some deviations from a perfect circular shape, obviously for the umbra, which has an internal structure. At the upper left, the penumbra is more extended than elsewhere.

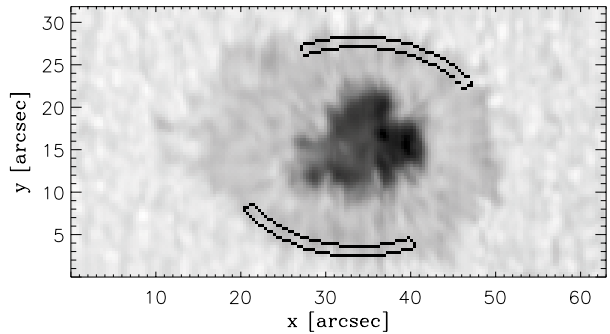


**Fig. 2.** Image of the spot composed from the Stokes-I spectra obtained during the scan. The surrounded areas in the outer penumbra are selected for the correlation analysis in section 5. The ordinate is parallel to the direction to disk centre.

As method for the inversion we use the SIR-code (Stokes Inversion based on Response functions) of Ruiz Cobo & del Toro Iniesta (1992). We restrict ourselves to a one-component model atmosphere, and we assume that the magnetic field and the Doppler velocities are constant over the height range where our line is formed. Besides the field strength, SIR yields also reliable results for the inclination and the azimuth of the magnetic field. After the inversion, the results are resized in the same way as the intensity data for the Figures.

## 3. Results

### 3.1. Size of penumbral filaments

A slice along a circular arc with a radius of 8850 km and a length of 33984 km was chosen for the computation of power spectra of the penumbral intensity fluctuations. To obtain a step width of 59 km we applied a cubic interpolation scheme to all slices. A cosine apodisation filter at the outer 10% removed the influence of non-periodic boundary conditions. The sampling rate of the raw data is higher than the resolution limit of the telescope, hence aliasing effects are not to be expected. Figure 3 shows the resulting temporally averaged power spectrum. This power spectrum reaches the noise level at wavenumber  $35 \text{ Mm}^{-1}$ , corresponding to 190 km.

In a simple model we assume that the penumbra is composed of structures of the same size with a constant width but with a random placement. A noise component is added, extrapolated from the observed power spectrum at wavenumbers above  $40 \text{ Mm}^{-1}$  (beyond the resolution limit of the telescope). Power spectra for such models with different intrinsic widths are computed. We obtain an excellent agreement between the observed power spectrum and that for an intrinsic width of 250 km. Curves for 220 and 290 km already show significant differences. A very similar result was derived by Sütterlin (2001) for a different spot. In that paper it is shown that the DOT is really able to resolve smaller structures than 250 km, for an area of ‘‘active granulation’’ the power remains higher around  $35 \text{ Mm}^{-1}$  than for penumbra structures. In our case we do not have ‘‘active granulation’’ inside our field of

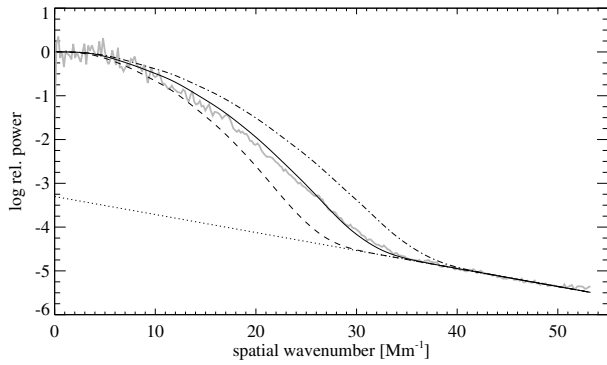


**Fig. 3.** Spatial power spectra for the penumbral intensity variations. The observed one is given by the thick grey line, the solid line represents the model with a typical width of 250 km, the dashed line stands for 290 and the dash-dotted line for 220 km. The straight dashed line shows the noise level.

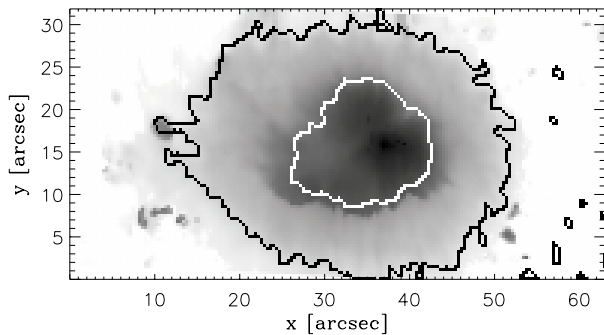


**Fig. 4.** Map of the magnetic field strength  $B$ . If the net polarization drops below a certain limit, the value of  $B$  is set to zero (white). The contours give the outer edge of the penumbra in the continuum and the umbra-penumbra boundary ( $0.83\% I_c$ ). Black corresponds to 3000 G.

view. A test in “normal granulation” only exhibits a somewhat higher noise level.

### 3.2. Magnetic field and Doppler velocities

Figure 4 shows a map of the magnetic field strength. The maximum value in the umbra is 2992 G. In the outer penumbra we find values between 800 and 1000 G. There is clearly polarization outside the penumbral boundary as seen in the continuum, the corresponding magnetic field strength is around 500 G or below. In Figure 1, the G-band image, we see many bright points just outside the penumbra. The general slope of the magnetic field follows the intensity contours of the spot, but we see a streak of higher magnetic field in the upper left part which is un conspicuous in the intensity.

Figure 5 shows the Doppler velocities. The Evershed flow varies between  $-3.5$  km/s and  $+3.5$  km/s. These velocities are quite high compared with former results, but there have been several indications that there are at least two components of the flow, one of them close to or even beyond the sound speed (see e. g. Wiehr 1995 or del Toro Iniesta et al. 2001).

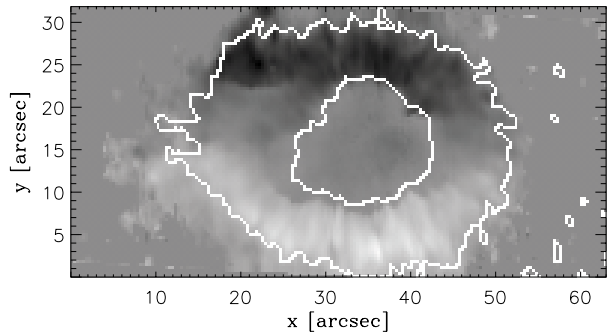


**Fig. 5.** Map of Doppler velocities. Velocities vary in a spectral sequence from  $-3.5$  km/s (towards observer, black) to  $+3.5$  km/s (white), grey indicates no or small Doppler shift.

**Table 1.** Correlation coefficients  $r$  for the relations between intensity  $I$ , magnetic field strength  $B$ , Doppler velocity  $v$  and magnetic inclination  $\gamma$ . Index c stands for centre-side, l for limb-side.

Quantities	$r_c$	$r_l$
I,B	-0.49	-0.76
I,v	+0.01	-0.55
I, $\gamma$	-0.09	-0.23
B,v	+0.19	+0.65
B, $\gamma$	-0.33	+0.38
v, $\gamma$	+0.51	+0.77

An important question is the relation between intensity structures and azimuthal variations of the magnetic field or Doppler velocities in the outer penumbra. To avoid influences from the general dependence of the physical quantities on the distance from the centre of the spot, we use the differences from the local mean instead of the quantities themselves for the correlation analysis. From these maps, values are extracted between elliptically limited sectors in the outer penumbra (see Figure 2). Since our spot shows deviations from a circular shape in the upper left part, we use only two opposite sectors of the spot ( $30^\circ - 120^\circ$  and  $210^\circ - 300^\circ$ ). Correlation coefficients are given in Table 1, and scatter plots are shown in Figure 6.

These results stand for a correlation between intensity structures and variations of the magnetic field and Doppler velocities, respectively, in the sense that brighter structures have less magnetic field and less Evershed flow. This tendency is more pronounced at the limb side. Velocities are higher in the more inclined magnetic field, while we obtain different signs of the correlations between magnetic field strength and inclination at the centre and the limb side. Correlations between intensity and magnetic inclination are rather low, in contrast to previous reports. Perhaps our spatial resolution of  $1''0$  is not high enough.

## 4. Conclusions

1. The comparison of the observed spatial power spectrum with our model calculations indicates that penumbral fila-

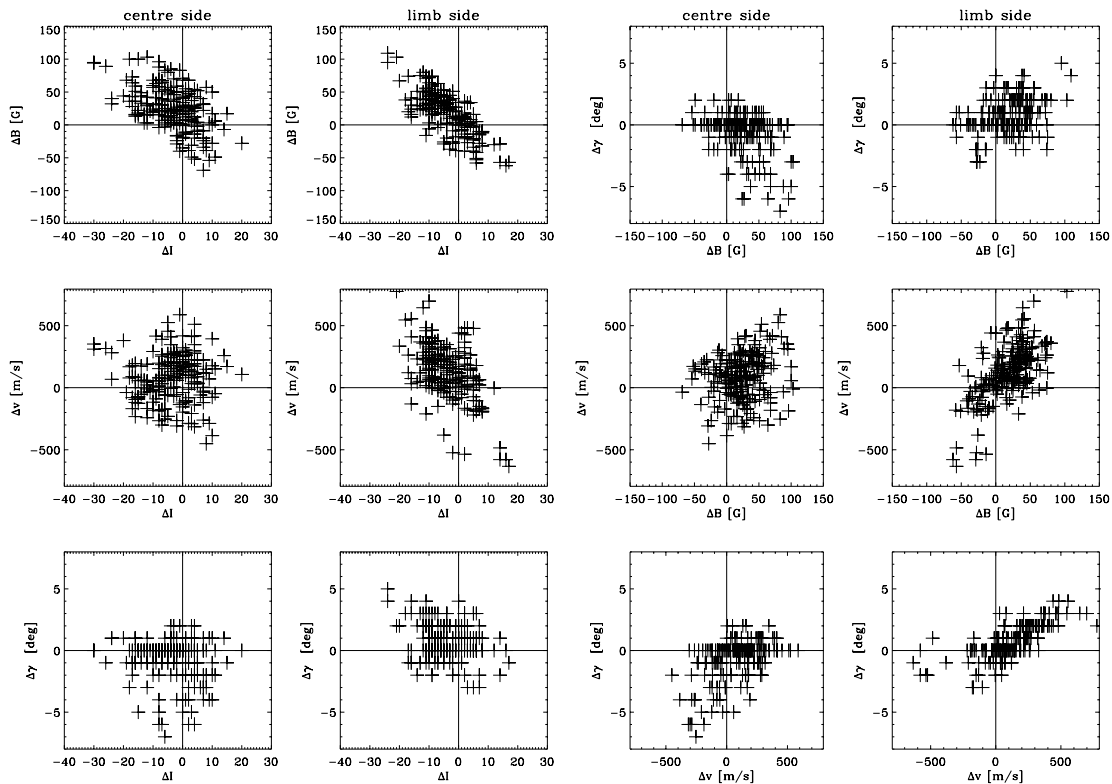


**Fig. 6.** Scatter plots for the relations of the variations of intensity and magnetic field (upper left panels), intensity and velocity (middle left panels), intensity and magnetic inclination (lower left panels), magnetic field strength and inclinations (upper right panels), magnetic field strength and velocities (middle right panels) and velocities and magnetic inclination (lower right panels). The first and third columns stand for the centre-side penumbra, the second and fourth for the limb-side penumbra.

ments have a typical width of 250 km, as already found by Sütterlin (2001). We cannot be sure that this disproves the MISMA concept of Sánchez Almeida (1998), but if that concept is correct it has to be explained why conglomerates of a size of 250 km are formed. A size of 250 km is large enough that filaments can survive for about an hour or even longer before they disappear due to radiative cooling as calculated by Schlichenmaier et al. (1999).

2. Magnetic field strength and Doppler velocities are correlated with intensity variations in the outer penumbra; dark structures show higher magnetic field and higher velocities. The correlation between intensities and magnetic inclination is insignificant.
3. Doubts remain on the correlations, because the spatial resolution of the VTT is not high enough at  $1.5 \mu\text{m}$  to resolve the penumbral fine structures with a size of 250 km. On the other hand, the high magnetic sensitivity in the IR is required to determine the magnetic finestructure. A larger telescope with an aperture of at least 1.5 m like GREGOR is needed.

*Acknowledgements.* One of us (H.B) is very grateful to the colleagues from the Instituto de Astrofísica de Canarias (IAC), especially Dr. L. Bellot Rubio, for the SIR-code and their help with it. We appreciate the assistance of Dr. K. Muglach during the observations and helpful discussions. This research is part of the TMR-ESMN (European Solar Magnetometry Network) supported by the European Commission. The Vacuum Tower Telescope in Tenerife is operated by the Kiepenheuer-Institut für Sonnenphysik (Germany)

in the Spanish Observatorio del Teide of the IAC. The Dutch Open Telescope project is funded by the University of Utrecht, the Netherlands Graduate School for Astronomy NOVA and the Netherlands Organization for Scientific Research NWO; it is operated in the Spanish Observatorio del Roque de los Muchachos of the IAC.

## References

- Balthasar, H., Collados, M., Muglach, K.: 2000, AN 321, 121  
 Beckers, J.M., Schröter, E.H.: 1968, Solar Phys. 4, 303  
 Degenhardt, D., Wiehr, E.: 1991, A&A 252, 821  
 del Toro Iniesta, J.C., Bellot Rubio, L.R., Collados, M.: 2001, ApJ 549, L139  
 Lites, B.W., Elmore, D.F., Seagraves, P., Skumanich, A. P.: 1993, ApJ 418, 928  
 Martínez Pillet, V.: 2000, A&A 361, 734  
 Martínez Pillet, V.: 2001, A&A 369, 644  
 Martínez Pillet, V., Collados, M., Sánchez Almeida, J., et al.: 1999, ASP Conf. Ser. 183, 264  
 Ruiz Cobo, B., del Toro Iniesta, J.C.: 1992, ApJ 398, 375  
 Sánchez Almeida, J.: 1998, ApJ 497, 967  
 Sánchez Almeida, J.: 2001, A&A 369, 643  
 Sánchez Almeida, J., Bonet J. A.: 1998, ApJ 505, 1010  
 Schlichenmaier, R., Jahn, K., Schmidt, H.U.: 1998, A&A 337, 897  
 Schlichenmaier, R., Bruls, J.H.M.J., Schüssler, M.: 1999, A&A 349, 961  
 Schmidt, W., Hofmann, A., Balthasar, H., Tarbell, T., Frank, Z.: 1992, A&A 264, L27  
 Stanchfield, D.C.H., Thomas, J.H., Lites, B.W.: 1997, ApJ 477, 485  
 Sütterlin, P.: 2001, A&A 374, L21  
 Wiehr, E.: 1995, A&A 298, L17